

Theory of Bose–Einstein condensation mechanism for deuteron-induced nuclear reactions in micro/nano-scale metal grains and particles

Yeong E. Kim

Received: 25 November 2008 / Revised: 2 February 2009 / Accepted: 2 April 2009 / Published online: 14 May 2009
© Springer-Verlag 2009

Abstract Recently, there have been many reports of experimental results which indicate occurrences of anomalous deuteron-induced nuclear reactions in metals at low energies. A consistent conventional theoretical description is presented for anomalous low-energy deuteron-induced nuclear reactions in metal. The theory is based on the Bose–Einstein condensate (BEC) state occupied by deuterons trapped in a micro/nano-scale metal grain or particle. The theory is capable of explaining most of the experimentally observed results and also provides theoretical predictions, which can be tested experimentally. Scalabilities of the observed effects are discussed based on theoretical predictions.

Keywords Bose–Einstein condensation · Deuteron fusion · Nuclear reactions · Metals

Introduction

Recently, experimental evidence for anomalous nuclear reactions have been observed in metals during Pd/D co-deposition experiments using a solid-state nuclear track detector, CR-39 (Szpak et al. 2005b, 2007; Mosier-Boss et al. 2007). Almost two decades ago, Fleischmann and Pons reported excess heat generation in electrolysis experiment using the negatively polarized Pd/D–D₂O system (Fleischmann and Pons 1989). Since then, many others have reported experimental observations of excess

heat generation and anomalous nuclear reactions occurring in metal at ultra-low energies (Storms and Talcott 1990, Storms 1993, 1996, McKubre et al. 1994, Bush et al. 1991, Miles et al. 1993, 1994, Lipson et al. 2000, Szpak et al. 1996, 1998, 2004, 2005a, b, 2007; Szpak and Mosier-Boss 1996; Mosier-Boss and Szpak 1999; Mosier-Boss et al. 2007; Arata and Zhang 2008). There have been reports of experimental results that heat (Szpak et al. 2004), γ -ray and/or X-ray radiation (Szpak et al. 1996), tritium (Szpak et al. 1998), and energetic particles (Szpak et al. 2007) are produced in bursts and sporadically in cathodes by Pd-D co-deposition. These anomalous reaction rates cannot be explained using the conventional theory of nuclear reactions in free space, which predicts extremely low nuclear reaction rates at ultra-low energies (≤ 10 eV) due to the Gamow factor arising from the Coulomb repulsion between two charged nuclei undergoing nuclear-reaction process.

In this paper, a consistent conventional theoretical description is presented for explaining the anomalous results observed for deuteron-induced nuclear reactions in metal at ultra-low energies (Fleischmann and Pons 1989; Storms and Talcott 1990, Storms 1993, 1996, McKubre et al. 1994, Bush et al. 1991, Miles et al. 1993, 1994, Lipson et al. 2000, Szpak et al. 1996, 1998, 2004, 2005a, b, 2007; Szpak and Mosier-Boss 1996; Mosier-Boss and Szpak 1999; Mosier-Boss et al. 2007; Arata and Zhang 2008). The theory presented in this paper is capable of explaining the above observations, and provides theoretical predictions which can be tested experimentally for the confirmation of the theory. A detailed description of the theoretical explanation, based on the theory of Bose–Einstein condensation nuclear fusion (BECNF; Kim et al. 1997, Kim and Zubarev 1998 (unpublished report), 2000a, b, 2001, 2002) and on selection rules recently derived for a mixed system

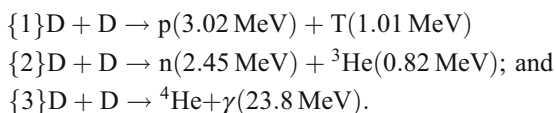
Y. E. Kim (✉)
Physics Department, Purdue University,
525 Northwestern Avenue,
West Lafayette, IN 47907, USA
e-mail: yekim@purdue.edu

of two species (Kim and Zubarev 2006), are presented along with suggested experimental tests of predictions of the theory and a discussion of the scalability of the fusion rates based on the theory.

Earlier experimental results were obtained using bulk Pd (rod or wire; Fleischmann and Pons 1989, Storms and Talcott 1990, Storms 1993, 1996, McKubre et al. 1994, Bush et al. 1991, Miles et al. 1993, 1994) or using Pd foils (Lipson et al. 2000). However, even bulk or foil metals will have micro-scale grains with boundaries created by impurities. Furthermore, electrolysis could create micro/nano-scale dendrites on the metal surface.

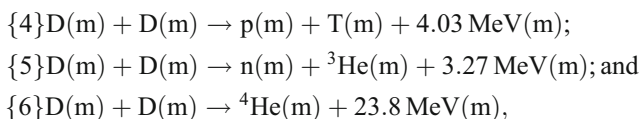
Summary of anomalous experimental results

The conventional deuterium fusion in free space proceeds via the following nuclear reactions:



The cross-sections (or reaction rates) for reactions {1}–{3} have been measured by beam experiments at intermediate energies (≥ 10 keV), and are expected to be extremely small at low energies (≤ 10 eV) due to the Gamow factor arising from Coulomb barrier between two deuterons. The measured cross-sections have branching ratios: $(\sigma\{1\}, \sigma\{2\}, \sigma\{3\}) \approx (0.5, 0.5, 10^{-6})$.

From many experimental measurements by Fleischmann and Pons 1989, and many others over 19 years since then (Storms and Talcott 1990, Storms 1993, 1996, McKubre et al. 1994, Bush et al. 1991, Miles et al. 1993, 1994, Lipson et al. 2000), including the recent work by Szpak, Mosier-Boss, Gordon et al. (Szpak et al. 1996, 1998, 2004, 2005a, b, 2007; Szpak and Mosier-Boss 1996; Mosier-Boss and Szpak 1999; Mosier-Boss et al. 2008), and the most recent work by Arata and Zhang (2008), the following experimental results have emerged. At ambient temperatures or low energies (≤ 10 eV), deuterium fusion in metal proceeds via the following reactions:



where m represents a host metal lattice or metal particle. Reaction rate R for {6} is dominant over reaction rates for {4} and {5}, i.e., $R\{6\} \gg R\{4\}$ and $R\{6\} \gg R\{5\}$. Additional experimental observations include requirements of both higher deuterium loading ($D/Pd \geq 1$) and deuterium purity ($H/D \ll 1$), the phenomenon of “heat after death”

(Szpak et al. 2004), and enhancement of the effect by electromagnetic fields (Szpak et al. 2005a, b; Mosier-Boss et al. 2007) and laser stimulation (Letts and Craven 2006, unpublished report).

Bose–Einstein condensation mechanism

The concept of the Bose–Einstein condensation (BEC; Bose 1924; Einstein 1924) has been known for 84 years, and has been used to describe all physical scales, including liquid ${}^4\text{He}$, excitons in semiconductors, pions and kaons in dense nuclear matter (neutron stars, supernovae), and elementary particles (Griffin et al. 1995). It was only 13 years ago in 1995 that the BEC phenomenon was observed directly in dilute vapors of alkali atoms, such as rubidium (Anderson et al. 1995), lithium (Bradley et al. 1995), and sodium (Davis et al. 1995) confined in magnetic traps and cooled down to nano Kelvin temperatures.

Atomic BEC vs. nuclear BEC

In the atomic BEC case (Anderson et al. 1995), the BEC state was created by cooling dilute Rb atoms loaded into a magnetic confinement potential at 300 K. It was cooled by laser cooling (Doppler cooling) to $\sim 90 \mu\text{K}$ (4×10^6 atoms) with a density of 2×10^{10} atoms/cm³. Further cooling was accomplished by evaporation cooling removing energetic atoms to 170 nK. At 170 nK, it consists of 2,000 atoms at a number density of 2.6×10^{12} /cm³ in BEC state (near zero velocity) while other 2×10^4 atoms in the trap had a Maxwell–Boltzmann (MB) velocity distribution with an exponential tail characteristic of $T \approx 170$ nK. The requirement for BEC, $\lambda_{\text{db}} > d$, is satisfied, where $\lambda_{\text{db}} \approx 8.2 \times 10^3 \text{ \AA}$ ($= 0.82 \mu\text{m}$) is the de Broglie wavelength and $d \approx 7.3 \times 10^3 \text{ \AA}$ ($= 0.73 \mu\text{m}$) is interatomic spacing distance.

In our nuclear BEC phenomenon, we have deuterium number density of $\sim 6.8 \times 10^{22}$ cm⁻³ in Pd metal, corresponding to an average separation distance of $d \approx 2.45 \text{ \AA}$ between deuterons. In order to achieve the nuclear BEC state of deuterons in metal, we need to have the average deuterium kinetic energy T_d smaller than $T_d^c = 0.0063$ eV, i.e. $T_d < T_d^c$ in order to satisfy the requirement $\lambda_{\text{db}} > d$.

Generalization of the MB distribution

The MB distribution is originally derived for weakly interacting dilute gas (ideal gas). For strongly interacting and dense systems such as mobile deuterons in metal, the MB distribution is not applicable and hence average deuterium kinetic energy of $kT = 0.026$ eV at $T = 300$ K is not applicable for deuterons in metal. There have been

theoretical efforts for generalization of the MB distribution. Two theoretical approaches (non-extensive statistical mechanics and quantum statistical mechanics) are described in the following two subsections. At present, there are no reliable experimental measurements and no reliable theoretical descriptions for determining the velocity distribution of deuterons in metals.

Non-extensive statistical mechanics

Although Maxwell–Boltzmann distribution derived from Boltzmann–Gibbs entropy describes well a many-body system in thermal equilibrium (or stationary state), it cannot describe other physical systems which are in thermal meta-equilibrium (quasi-stationary state). Most of the physical many-body systems we encounter in nature are not in thermal equilibrium but are in thermal meta-equilibrium. In 1988, non-extensive statistical mechanics was developed by Tsallis (1988) as a generalization of the Boltzmann–Gibbs entropy and standard statistical mechanics. One of the distinct features of the non-extensive statistical mechanics (Tsallis 1988; Gell-Mann and Tsallis 2004) is a power-law distribution tail instead of the exponential tail of the Maxwell–Boltzmann distribution. Applications of the non-extensive statistical mechanics to many different fields (physics, chemistry, biology, economics, linguistics, medicine, geophysics, cognitive sciences, computer sciences, and social sciences) are currently being carried out (Gell-Mann and Tsallis 2004).

Quantum statistical mechanics

For strongly interacting and dense systems, the MB distribution needs to be modified by quantum statistical mechanics. In 1959, Martin and Schwinger developed nonperturbative theory of many-particle systems based on quantum-field theoretic techniques using thermodynamic Green's function (Martin and Schwinger 1959). More detailed description of the Green's function theory along the lines of the work of Martin and Schwinger (1959) is given in the book “Quantum Statistical Mechanics” by Kadanoff and Baym (1962).

Based on earlier works on quantum-field theoretic techniques developed by Galitskii and Migdal (1958) and Galitskii (1958) in 1958 (see also the book by Abrikosov et al. (1963)), Galitskii and Yakimets (GY) (1966) showed that the quantum energy indeterminacy due to interactions between particles in a plasma (National Research Council 1995; we adopt the definition of “plasma” in this report) leads to a generalized momentum distribution which has a high-energy momentum distribution tail diminishing as an inverse eighth power of the momentum, instead of the conventional Maxwell–Boltzmann distribution tail decay-

ing exponentially. Recently, Kim and Zubarev (2006b; 2007a, b) found the effect of the GY momentum distribution for the deuteron plasma fusion rates is unexpectedly very large in comparison with results obtained using the conventional Maxwell–Boltzmann momentum distribution for the deuteron plasma nuclear fusion rate. This result may have very important implications not only for the theoretical aspects but also for practical applications for clean nuclear fusion energy generation.

Deuteron mobility and BEC in metals

There are experimental evidence (Coehn 1929; Coehn and Specht 1930; Duhm 1935; Barer 1941; Marcheche et al. 1976; Lewis 1982; Fukai 2005) that heating and/or applying an electric field in a metal causes hydrogens and deuterons in a metal to become mobile, thus leading to a higher density for quasi-free mobile deuterons in a metal. It is expected that the number of mobile deuterium ions will increase, as the loading ratio D/metal of deuterium atoms increases and becomes larger than one, $D/metal \geq 1$.

Mobility of deuterons in a metal is a complex phenomenon and may involve a number of different processes (Fukai 2005): coherent tunneling, incoherent hopping, phonon-assisted processes, thermally activated tunneling, and over-barrier jump/fluid like motion at higher temperatures. Furthermore, applied electric fields as in electrolysis experiments can enhance the mobility of absorbed deuterons.

If the number density of mobile deuterons in the metal (Pd) can be increased to a comparable density of metal atoms (Pd), the average distance, d , between the mobile deuterons can be substantially reduced. This may provide an alternative experimental technique for achieving the BEC requirement, $\lambda_{db} > d$, by increasing mobile deuteron density (thus reducing d), rather than cooling mobile deuterons (for increasing λ_{db}), as was done in the atomic BEC experiments.

If mobile deuterons in a metal are confined by a confining potential provided by metal atoms and electrons, it may be possible that deuteron momentum or velocity distribution in a metal may have the average deuteron kinetic energy smaller than $T_d^c = 0.0063$ eV, thus satisfying $\lambda_{db} > d$. We note that $T_d^c = 0.0063$ eV corresponds to the average deuteron velocity of $v_c = 0.78 \times 10^5$ cm/s while the average deuteron kinetic energy of $kT = 0.026$ eV with $T = 300$ K corresponds to the average deuteron velocity of $v_k = 1.6 \times 10^5$ cm/s. Boundaries for micro/nano-scale metal grains and particles can act as barriers and may slow down mobile deuterons resulting in lower average velocity $v_d < v_c$ and smaller average kinetic energy $T_d < T_d^c$ near boundaries. Therefore, it may be possible that the conditions, $T_d < T_d^c$ and $\lambda_{db} > d$, are achieved for mobile deuterons in

localized regions of the metal without cooling as done in the atomic BEC case, and hence, it may be possible to observe experimentally the effects of the nuclear BEC.

Theory of Bose–Einstein condensation nuclear fusion (BECNF)

Theoretical formulation for single species case

For applying the concept of the BEC mechanism to deuteron fusion in a nano-scale metal particle, we consider N identical charged Bose nuclei (deuterons) confined in an ion trap (or a metal grain or particle). Some fraction of trapped deuterons is assumed to be mobile as discussed above. The trapping potential is three-dimensional (nearly-sphere) for nano-scale metal particle, or quasi two-dimensional (nearly hemi-sphere) for micro-scale metal grains, both having surrounding boundary barriers. The barrier heights or potential depths are expected to be an order of energy (≤ 1 eV) required for removing a deuteron from a metal grain or particle. For simplicity, we assume an isotropic harmonic potential for the ion trap to obtain order of magnitude estimates of fusion reaction rates.

N -body Schroedinger equation for the system is given by

$$H\Psi = E\Psi \quad (1)$$

with the Hamiltonian H for the system given by

$$H = \frac{\hbar^2}{2m} \sum_{i=1}^N \Delta_i + \frac{1}{2} m \omega^2 \sum_{i=1}^N r_i^2 + \sum_{i < j} \frac{e^2}{|r_i - r_j|} \quad (2)$$

where m is the rest mass of the nucleus. Only two-body interactions (Coulomb and nuclear forces) are considered since we expect that three-body interactions are expected to be much weaker than the two-body interactions. Multi-body effects described in the following are due to the correlated many-body state described by the BEC state.

The approximate solution of Eq. (1) for the ground state is obtained using the equivalent linear two-body method (Kim and Zubarev 2001, 2002). The use of an alternative method based on the mean-field theory for bosons yields the same result (see Appendix in Kim and Zubarev 2000b). Based on the optical theorem formulation of low-energy nuclear reactions (Kim et al. 1997), the ground state solution is used to derive the approximate theoretical formula for the deuteron–deuteron fusion rate in an ion trap (micro/nano-scale metal grain or particle). The detailed derivations are given elsewhere (Kim and Zubarev 2000a, b).

Our final theoretical formula for the nuclear fusion rate R_{trap} for a single trap containing N deuterons is given by

$$R_{\text{trap}} = \Omega B N \omega^2 \quad (3)$$

with

$$\omega^2 = \sqrt{\frac{3}{4\pi}} \alpha \left(\frac{\hbar c}{m} \right) \frac{N}{\langle r \rangle^3} \quad (4)$$

where $\langle r \rangle$ is the radius of trap/atomic cluster, $\langle r \rangle = \langle \Psi | r | \Psi \rangle$, N is the average number of Bose nuclei in a trap/cluster, and B is given by $B = 3 A m / (8 \pi \alpha \hbar c)$, with $A = 2 S r_B / (\pi \hbar)$, $r_B = \hbar^2 / (2 \mu e^2)$, and $\mu = m / 2$. S is the S-factor for the nuclear fusion reaction between two deuterons. For D(d,p)T and D(d,n)³He reactions, we have $S \approx 55$ keV-barn. We expect also $S \approx 55$ keV-barn for reaction {6}. Only one unknown parameter is the probability of the BEC ground state occupation, Ω . It may be proportional to $N^{-1/3}$, $\Omega \propto N^{-1/3}$, or to N^{-2} , $\Omega \propto N^{-2}$.

We can rewrite Eq. (3) as

$$R_{\text{trap}} = 4(3/4\pi)^{3/2} \Omega A \frac{N^2}{D_{\text{trap}}^3} \propto \Omega \frac{N^2}{D_{\text{trap}}^3} \quad (5)$$

where $A = 0.77 \times 10^{-16} \text{ cm}^3/\text{s}$ and D_{trap} is the average diameter of the trap, $D_{\text{trap}} = 2 \langle r \rangle$.

The total fusion rate R_t is given by

$$R_t = N_{\text{trap}} R_{\text{trap}} = \frac{N_D}{N} R_{\text{trap}} \propto \Omega \frac{N}{D_{\text{trap}}^3} \quad (6)$$

where N_D is the total number of deuterons and $N_{\text{trap}} = N_D / N$ is the total number of traps. Eq. (6) shows that the total fusion rates, R_t , are not necessarily slow if Ω is not extremely small.

Two species case

We consider a mixture of two different species of positively charged nuclear particles, labeled 1 and 2, with N_1 and N_2 particles, respectively, both trapped in a micro/nano-scale metal grain or particle. We denote charges and masses as $Z_1 \geq 0$, $Z_2 \geq 0$, and m_1 , m_2 , respectively. The detailed derivations are given in reference (Kim and Zubarev 2006a, unpublished report). A brief outline of the derivation is given below.

We assume that trapping potentials, V_i , are isotropic and harmonic $V_i(\vec{r}) = m_i \omega_i^2 r^2 / 2$. We use the mean-field theory (Esry 1997; Kim and Zubarev 2001) for a system of interacting bosons confined in a harmonic potential. The mean-field energy functional for the two-component system is given by generalization of the one-component case

$$E = \sum_{i=1}^2 E_i + E_{\text{int}}, \quad (7)$$

where

$$E_i = \int d\vec{r} \frac{\hbar^2}{2m_i} |\nabla \psi_i|^2,$$

$$E_{\text{int}} = \frac{e^2}{2} \int d\vec{x} d\vec{y} \frac{(Z_1 n_1(\vec{x}) + Z_2 n_2(\vec{x}))(Z_1 n_1(\vec{y}) + Z_2 n_2(\vec{y}))}{|\vec{x} - \vec{y}|}, \tag{8}$$

and n_i denotes density of specie i , $n_i = |\psi_i|^2$, and $\int d\vec{r} n_i(\vec{r}) = N_i$. In Eq. (7), we have neglected effects of order $1/N_i$.

The minimization of the energy functional, Eq. (7), with subsidiary conditions, Eq. (8), leads to the following time-independent mean-field equations,

$$-\frac{\hbar^2}{2m_i} \nabla^2 \psi_i(\vec{r}) + (V_i + W_i) \psi_i(\vec{r}) = \mu_i \psi_i(\vec{r}), \tag{9}$$

where

$$W_i(\vec{r}) = e^2 \int d\vec{y} [Z_1^2 n_1^2(\vec{y}) + Z_1 Z_2 n_1(\vec{y}) n_2(\vec{y})] / (|\vec{r} - \vec{y}| n_i(\vec{y})), \tag{10}$$

and μ_i are the chemical potentials, which are related to the ground state energy, Eq. (7), by the general thermodynamics identity $\mu_i = \partial E / \partial N_i$.

In the Thomas–Fermi (TF) approximation, in which one neglects the kinetic energy terms in Eq. (9), Eq. (9) reduces to

$$\mu_i = V_i + W_i. \tag{11}$$

Equation (11) holds in the region where n_i are positive and $n_i=0$ outside this region.

Selection rule

For the BEC mechanism, we now derive the nuclear charge-mass selection rule (approximate). We can obtain from Eq. (11) that

$$\mu_2 - \frac{Z_2}{Z_1} \mu_1 = \left(\frac{m_2 \omega_2^2}{m_1 \omega_1^2} - \frac{Z_2}{Z_1} \right) \frac{m_1 \omega_1^2}{2} r^2. \tag{12}$$

Since μ_i are independent of r , Eq. (12) leads to the conclusion that Eq. (11) has non-trivial solution if and only if

$$\left(\frac{m_2 \omega_2^2}{m_1 \omega_1^2} - \frac{Z_2}{Z_1} \right) = 0, \tag{13}$$

If we assume $\omega_1 = \omega_2$, we obtain from Eq. (13) the following selection rule:

$$\frac{Z_1}{m_1} = \frac{Z_2}{m_2} \tag{14}$$

We now apply the selection rule, Eq. (14). If we use m as mass number approximately given in units of the nucleon mass, we have $[Z_1(\text{D})/m_1(\text{D})] = 1/2$, $[Z_2(\text{p})/m_2(\text{p})] = 1$, $[Z_2(\text{T})/m_2(\text{T})] = 1/3$, $[Z_2(\text{n})/m_2(\text{n})] = 0$, and $[Z_2(^3\text{He})/m_2(^3\text{He})] = 2/3$

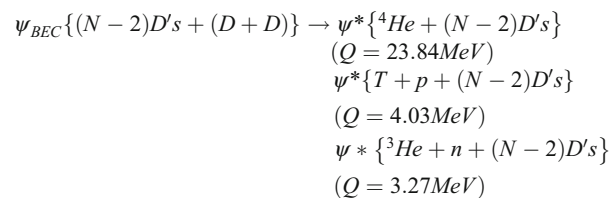
Since $[Z_1/m_1] \neq [Z_2/m_2]$ for reactions {4} and {5} they are forbidden or suppressed, and fusion reaction rates for reactions {4} and {5} are expected to be small, while reaction {6} is allowed since $[Z_1/m_1] = [Z_2/m_2]$, and fusion reaction rate is expected to be large for reaction {6}. In summary, we obtain $R\{6\} \gg R\{4\}$ and $R\{6\} \gg R\{5\}$.

Theoretical implications

Eqs. (3) and (6) provide an important result that nuclear fusion rates R_{trap} and R_t do not depend on the Gamow factor in contrast to the conventional theory for nuclear fusion in free space. This could provide explanations for overcoming the Coulomb barrier and for the claimed anomalous effects for low-energy nuclear reactions in metals.

This is consistent with the conjecture noted by Dirac (1935) and used by Bogolubov (1966) that boson creation and annihilation operators can be treated simply as numbers when the ground state occupation number is large. This implies that for large N , each charged boson behaves as an independent particle in a common average background potential and the Coulomb interaction between two charged bosons is suppressed.

For a single trap (or metal particle) containing N deuterons, the deuteron–deuteron fusion can proceed with the following three reaction channels.



where ψ_{BEC} is the Bose–Einstein condensate ground state (a coherent quantum state) with N deuterons and ψ^* are final excited continuum states. Excess energy (Q value) is absorbed by the BEC state and shared by $(N-2)$ deuterons and reaction products in the final state.

In addition to 2D fusion channel described above, 3D and 4D fusion channels are possible. However, probabilities for 3D and 4D fusions are expected to be much smaller than that of 2D fusion.

We now consider the total momentum conservation. The initial total momentum of the initial BEC state with N deuterons (denoted as D^N) is given by $\vec{P}_{D^N} \approx 0$. Because of the total momentum conservation, the final

total momenta for reactions {4}, {5}, and {6} are given by

$$\begin{aligned} \{4\} \vec{P}_{D^{N-2}pT} &\approx 0, \langle T_D \rangle \approx \langle T_p \rangle \approx \langle T_T \rangle \approx Q\{4\}/N \\ \{5\} \vec{P}_{D^{N-2}n^3He} &\approx 0, \langle T_D \rangle \approx \langle T_n \rangle \approx \langle T_{^3He} \rangle \approx Q\{5\}/N \\ \{6\} \vec{P}_{D^{N-2}n^4He} &\approx 0, \langle T_D \rangle \approx \langle T_{^4He} \rangle \approx Q\{6\}/N \end{aligned}$$

where T represents the kinetic energy.

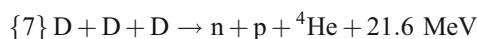
For a micro-scale metal grain confined by grain boundaries of $\sim 1 \mu\text{m}$ diameter, we expect to have $N \approx 10^{10}$ and $Q\{6\}/N \approx 10^{-3} \sim 10^{-4} \text{eV}$, and hence we expect the excess heat and ^4He production due to reaction {6} but no nuclear ashes from some of the reactions described below in the next section.

For nano-scale metal particles, the above consideration shows that excess energies (Q) lead to a micro/nano-scale fire-work type explosion, creating a crater/cavity and a hot spot with fire-work-like star tracks. This prediction is consistent with the results reported by Szpak and Mosier-Boss (1996). The size of a crater/cavity will depend on number of neighboring Pd nanoparticles participating in BEC fusion almost simultaneously. Since sizes of deuteron and Pd nucleus are of the order of $\sim 10^{-4} \text{A}$ ($\sim 10 \text{fm}$) while the average distance between two neighboring Pd atoms is $\sim 2.5 \text{A}$, $\sim 10 \text{keV}$ (up to 23.8MeV) deuteron from the BEC deuterium fusion encounters mostly electrons and transfers its kinetic energy to electrons and may induce X-rays, γ -rays, and Bremsstrahlung X-rays. Occasionally, $\sim 10 \text{MeV}$ (up to 23.8MeV) deuteron may interact with Pd nucleus to initiate nuclear reactions, Pd(d,p)Rh, etc. When the BEC deuterium fusion takes place in a Pd nanoparticle, exploding deuterons are expected to damage and leave the host Pd nanoparticle, but some of the Pd nanoparticles may remain intact and may participate again in the BEC deuterium fusion after absorbing again a sufficient number of deuterons, $D/\text{Pd} \geq 1$.

Theoretical Prediction

Effects due to deuterons

Deuterons with $Q\{6\}/N \approx \sim 10 \text{keV}$ (up to 23.8MeV) energy from reaction {6} can undergo reactions {1} and {2} producing p(3.02MeV), T(1.01MeV), n(2.45MeV), and ^3He (0.82MeV), and also interact with surrounding deuterons via the following reaction {7}.



Reaction {7} will produce neutrons with a maximum kinetic energy of $\sim 18 \text{MeV}$.

Tritons produced by reaction {1} (1.01MeV triton) and by reaction {4} (average kinetic energy of $Q\{4\}/N \approx \sim \text{keV}$)

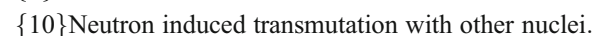
will interact with surrounding deuterons via the following reaction



Because of triton kinetic energies of 1.01MeV or $\sim \text{keV}$, the reaction rate for {8} could be large enough to produce 14.07-MeV neutrons. Neutrons from reaction {7} and/or {8} may have been recently observed by Mosier-Boss et al. (2008). We note that ^4He produced by reactions {7} and {8} have much high kinetic energies.

Effects due to neutrons

Neutrons with 2.45MeV kinetic energy from reaction {2}, neutrons with $Q\{5\}/N \approx \sim \text{keV}$ kinetic energy from reaction {5}, or neutrons from reactions {7} and {8} can undergo further reactions, {9} and/or {10} below:



In addition, energetic neutrons from reactions {7} or {8} may initiate reactions, $^{12}\text{C}(n,n')^3 ^4\text{He}$ and $^{12}\text{C}(n,n'\alpha)^8\text{Be}$ ($^8\text{Be} \rightarrow 2^4\text{He}$), which may have been recently observed by Mosier-Boss et al. (2008).

Since reaction {9} produces more tritiums than neutrons, we expect $R(T) > R(n)$, and also $R(T) > R(^3\text{He})$.

High deuterium loading requirement

The mobility of deuterons is required for the BEC mechanism. High loading ratio D/Pd is required for deuteron mobility.

Deuterium purity requirement

Because of violation of the selection rule, $[Z_1(D)/m_1(D)] \neq [Z_2(p)/m_2(p)]$, presence of hydrogens in deuteriums will suppress the formation of the BEC states, thus diminishing the fusion rate due to the BEC mechanism. The required H/D ratio is expected to be $H/D < N^{-1}$. For a 5-nm Pd nanoparticle with $N \approx 10^3$, $H/D < 10^{-3}$, and hence 99.9% deuterium purity is required.

Heat after death

There have been observations of continued heat generation after the input for experiment is switched off. This effect is known as “heat after death” (Szpak et al. 2004). Because of mobility of deuterons in Pd particle traps, a system of $\sim 10^{22}$ deuterons contained in $\sim 10^{18}$ Pd particle traps (in 3g of Pd particles with average particle diameter of $\sim 50 \text{Å}$) is a dynamic system. When the experiment is switched off,

slow decay of normal loading occurs, and hence BEC states are continuously diminished to a small fraction of the $\sim 10^{18}$ Pd particle traps and undergo BEC fusion processes at slower rates, until the formation of the BEC state ceases or becomes negligible.

Enhancement by electromagnetic fields and laser stimulation

Application of electromagnetic fields (Szpak et al. 2005a, b; Mosier-Boss et al. 2007) and laser stimulation (Letts and Craven 2006, unpublished report) have been shown to enhance the excess heat production and other anomalous effects. These effects may be due to a decrease of the average kinetic energy of mobile deuterons and/or to an increase of mobile deuterons participating in the BEC fusion processes, since EM fields including alternating electric currents and lasers can affect the effective velocity of deuterons, either directly or indirectly.

Increase of resistance

When the BECNF occurs, more mobile deuterons will be created. This in turn will increase the resistance of metal. This effect may have been recently observed by Celani et al. (2008, unpublished report) in deuterium gas-loading experiments with Pd nanoparticles coated on a Pd wire.

Experimental tests of theoretical predictions

The first experimental test of the BEC mechanism for deuterium fusion with nano-scale Pd particles was carried out with Pd blacks loaded by high-pressure deuterium gas (Kim et al. 2003, unpublished report). The result of this experiment shows no excess heat production. This may be due to the fact that Pd nanoparticles (Pd Blacks) used had too large sizes (80–180 nm) and were clumped together (not isolated). The recent report of deuterium gas-loading experiment by Arata and Zhang (2008) show positive results of observing excess heat and ^4He production using ~ 5 nm Pd particles imbedded in ZrO_2 and purified deuterium. For experimental tests of the predictions of the theory, it would be advantageous scientifically to use samples of Pd nanoparticles deposited on thin films such as $\text{Al}_2\text{O}_3/\text{NiAl}(111)$ (Hansen et al. 1999; Shaikhutdinov et al. 2002; Morkel et al. 2005), even though bulk materials such as Pd nanoparticles imbedded in SiO_2 aerogels (Kim et al. 2006, unpublished report) are more suitable for practical applications. Other possibilities are to use other metals such as Zr or Ti nanoparticles. In all cases, the theory requires that metal nanoparticles and micrograins are to be separated from each other by boundaries.

Direct diagnostic experimental tests require the use of nano-structured metal particles fabricated with pre-specified dimensions. In addition to the previous experimental techniques used, basic experimental tests of BECNF predictions can also be carried out at ultra-high pressures using a diamond anvil cell (DAC), which can compress a small sample of deuterium-loaded metal (Pd, Ti, Zr, etc.) by applying ultra-high pressures up to ~ 3 million atmospheres.

Tests based on the average size of metal particles

From Eq. (6) with $N = N_D(\pi/6)D_{\text{trap}}^3$, we obtain $R_t(D_{\text{trap}}) \propto D_{\text{trap}}^{-1}$ or D_{trap}^{-6} , where D_{trap} is the average trap diameter, assuming $\Omega \propto N^{-1/3}$ or N^{-2} , respectively. This can be tested experimentally. This result provides a theoretical justification for using 50 Å Pd nanoparticles to maximize the total fusion rates.

Tests based on the temperature dependence

Since the probability Ω of the BEC ground state occupation increases at lower temperatures ($\Omega \approx 1$ near $T \approx 0$), the total fusion rate R_t will increase at lower temperatures, $R_t(T_{\text{low}}) > R_t(T_{\text{high}})$. However, R_t is proportional to N_D where N_D is the total number of mobile deuterons. Since $N_D(T_{\text{low}}) < N_D(T_{\text{high}})$, we expect $R_t[N_D(T_{\text{low}})] < R_t[N_D(T_{\text{high}})]$. The above opposite temperature dependences for R_t will complicate analysis of the temperature dependence of R_t .

Tests for reaction products and heat after death

Some examples of this type of tests are (1) to look for micro/nano-scale craters/cavities and hot spots with micro/nano-scale fire-work like star tracks at Pd nanoparticle sites, before and after death, and (2) to measure neutron energies to check the reaction products carries kinetic energies of 2.45 MeV from the secondary reaction {2}, and $Q\{5\}/N \approx \sim \text{keV}$ from reaction {5}.

Tests for increase of resistance

The resistance increase, as predicted by BECNF process, was successfully observed by Celani's group (2008, unpublished data). Further experimental tests of this type are needed.

Tests for scalability

One example is a scalability test based on the total number of N_{trap} . Since we have $R_t \propto N_{\text{trap}}$ for the same R_{trap} , we have theoretical prediction, $R_t(30\text{gPdparticles})/R_t(3\text{gPdparticles}) \approx 10$, etc., which can be tested experimentally.

Summary and conclusions

Theory of the BEC mechanism described in this paper provides a consistent conventional theoretical description of the results of many experimental works started by Fleischmann and Pons 1989 and by many others since then (Storms and Talcott 1990, Storms 1993, 1996, McKubre et al. 1994, Bush et al. 1991, Miles et al. 1993, 1994, Lipson et al. 2000), including the recent work of Szpak, Mosier-Boss, Gordon et al. (Szpak et al. 1996, 1998, 2004, 2005a, b, 2007; Szpak and Mosier-Boss 1996; Mosier-Boss and Szpak 1999; Mosier-Boss et al. 2007) and the most recent work of Arata and Zhang (2008). Theory is based on the concept of nuclear Bose–Einstein condensate state for mobile deuterons trapped in a micro/nano-scale metal grain or particle, which acts as a confinement or trapping potential, similar to a magnetic trap used to observe the atomic BEC phenomenon with atoms in 1995 (Anderson et al. 1995; Bradley et al. 1995; Davis et al. 1995). To validate this new concept of the nuclear BEC phenomenon, experimental tests for a set of key theoretical predictions are proposed. Scalabilities of the observed effects are also discussed.

References

- Abrikosov AA, Gorkov LP, Dzyaloshinski IE (1963) *Methods of quantum field theory in statistical physics* (revised English edition translated by R.A. Silverman). Dover, New York
- Anderson MH, Ensher JR, Matthews MR, Wieman CE, Cornell EA (1995) Observation of Bose–Einstein condensation in a dilute atomic vapor. *Science* 269:198–201
- Arata Y, Zhang YC (2008) The establishment of solid nuclear fusion reactor. *J. High Temp. Soc* 34(2):85–94
- Barer QM (1941) *Diffusion in and through solids*. Cambridge University Press, New York, NY
- Bogolubov N (1966) On the theory of superfluidity. *J Phys* 11:23–29
- Bose SN (1924) Planck's law and the light quantum hypothesis. *Z Phys* 26:178–181
- Bradley CC, Sackett CA, Tollett JJ, Hulet RG (1995) Evidence of Bose–Einstein condensation in an atomic gas with attractive interactions. *Phys Rev Lett* 75:1687–1690
- Bush B, Lagowski JJ, Miles MH, Os GS (1991) Helium production during the electrolysis of D₂O in cold fusion. *J Electroanal Chem* 304:271
- Coehn A (1929) Proof of the existence of protons in metals (with discussion). *Z Electrochem* 35:676–680
- Coehn A, Specht W (1930) Ueber die Beteiligung von Protonen an der Elektrizitätsleitung in Metallen (Role of protons in electric conductivity of metals). *Z Phys* 83:1–31
- Davis KB, Mewes M–O, Andrews MR, Van Druten NJ, Durfee DS, Kurn DM, Ketterle W (1995) Bose–Einstein condensation in a gas of sodium atoms. *Phys Rev Lett* 75:3969–3973
- Dirac PAM (1935) *The Principles of Quantum Mechanics*. second edition, Clarendon Press, Oxford Chapter XI, Section 62.
- Duhm B (1935) Diffusion of hydrogen in palladium. *Z Phys* 94:435–456
- Einstein A (1924) Quantentheorie des einatomigen idealen Gases (Quantum theory of monoatomic ideal gasses). *Sitz. Preuss Akad. Wiss.*:261–267
- Esry BD (1997) Hartree–Fock theory for Bose–Einstein condensates and the inclusion of correlation effects. *Phys Rev A* 55:1147–1159
- Fleischmann M, Pons S (1989) Electrochemically induced nuclear fusion of deuterium. *J. Electroanal. Chem.* 261:301–308; Errata (1989) *J. Electroanal. Chem.* 263:187
- Fukai Y (2005) *The Metal–Hydrogen System*, 2nd edn. Springer, Berlin
- Galitskii VM (1958) The energy spectrum of non-ideal Fermi-gas. *Sov Phys* 7:104–112
- Galitskii VM, Migdal AB (1958) Application of quantum field theory methods to the many-body problem. *Sov Phys JETP* 7:96–104
- Galitskii VM, Yakimets VV (1966) Particle relaxation in a Maxwell gas. *Zh. Eksp. Teor.* 51:957–961 [(1967) *JETP*; 24:637–641].
- Gell-Mann M, Tsallis C (eds) (2004) *Non-Extensive Entropy-Interdisciplinary Applications*. Oxford University Press, Oxford
- Griffin A, Snoke DW, Stringari S (1995) *Bose–Einstein Condensation*. Cambridge University Press, New York, NY
- Hansen KH, Worren T, Stempel S, Laegsgaard E, Baumer M, Freund H–J, Besenbacher F, Stensgaard I (1999) Palladium nanocrystals on Al₂O₃: structure and adhesion energy. *Phys Rev Lett* 83:4120–4123
- Kadanoff LP, Baym G (1962) *Quantum Statistical Mechanics*. Benjamin, New York, Chapters 1–4
- Kim YE, Zubarev AL (2000a) Nuclear fusion for Bose nuclei confined in ion traps. *Fusion Technology* 37:151–156
- Kim YE, Zubarev AL (2000b) Ultra low-energy nuclear fusion of Bose nuclei in nano-scale ion traps. *Italian Physical Society Proceedings* 70:375–384
- Kim YE, Zubarev AL (2001) Ground state of charged bosons confined in a harmonic trap. *Physical Review A* 64:013603–013603-6
- Kim YE, Zubarev AL (2002) Equivalent linear two-body method for Bose–Einstein condensates in time-dependent harmonic traps. *Physical Review A* 66:053602–053602-7
- Kim YE, Zubarev AL (2006) Effect of a generalized particle momentum distribution on plasma nuclear fusion rates. *Jpn J Appl Phys* 45:L452–L455
- Kim YE, Zubarev AL (2007a) Theoretical interpretation of anomalous enhancement of nuclear reaction rates observed at low energies with metal targets. *Jpn J Appl Phys* 46:1656–1662
- Kim YE, Zubarev AL (2007b) Quantum plasma nuclear fusion theory for anomalous enhancement of nuclear reaction rates observed at low energies with metal targets. *Proceedings of the International Nuclear Physics Conference, Tokyo, Japan, June 3–8, 2007* (to be published by Japanese Physical Society)
- Kim YE, Kim YJ, Zubarev AL, Yoon JH (1997) Optical theorem formulation of low-energy nuclear reactions. *Physical Review C* 55:801–809
- Lewis FA (1982) Palladium–hydrogen system 2. *Platinum Met. Rev* 26:20–27 70:78, 121–128
- Lipson AG, Lyakhov BF, Roussetski AS, Akimoto T, Mizuno T, Asami N, Shimada R, Miyashita S, Takahashi A (2000) Evidence for low-intensity D–D reaction as a result of exothermic deuterium desorption from Au/Pd/PdO:D heterostructure. *Fusion Technol* 38:238
- Marcheche JF, Rat J–C, Herold A (1976) Study of hydrogen-metal systems: potential induced by the diffusion of hydrogen in palladium. *J Chim Phys Phys Chim Biol* 73:983–987
- Martin PC, Schwinger J (1959) Theory of many-particle systems I. *Phys Rev* 115:1342–1373

- McKubre MCH, Crouch-Baker S, Rocha-Filho RC, Smedley SI, Tanzella FL (1994) Isothermal flow calorimetric investigations of the D/Pd and H/Pd systems. *J Electroanal Chem* 368:55
- Miles MH, Hollins RA, Bush BF, Logowski JJ, Miles RE (1993) Correlation of excess power and helium production during D₂O and H₂O electrolysis using palladium cathodes. *J Electroanal Chem* 346:99
- Miles MH, Bush B, Lagowski JJ (1994) Anomalous effects involving excess power, radiation and helium production during D₂O electrolysis using palladium cathodes. *Fusion Technol* 25:478
- Morkel M, Rupprechter G, Freund H-J (2005) Finite size effects on supported Pd nanoparticles: interaction of hydrogen with CO and C₂H₄. *Surf Sci* 588:L209–L219
- Mosier-Boss PA, Szpak S (1999) The Pd/ⁿH system: transport processes and development of thermal instabilities. *Nuovo Cim Soc Ital Fis A* 112:577–587
- Mosier-Boss PA, Szpak S, Gordon FE, Forsley LPG (2007) Use of CR-39 in Pd/D Co-deposition experiments. *Eur Phys J Appl Phys* 40:293–303
- Mosier-Boss PA, Szpak S, Gordon FE, Forsley LPG (2008) Triple tracks in CR-39 as the result of Pd-D Co-deposition: evidence of energetic neutrons. *Naturwissenschaften* doi:10.1007/s00114-008-0449-x
- National Research Council (1995) *Plasma Science*. National Academy Press, Washington, D.C, p 1
- Shaikhutdinov Sh, Helmeier M, Hoffmann J, Meusel I, Richter B, Baumer M, Kuhlbeck H, Libuda J, Freund H-J, Oldman R, Jackson SD, Konvicka C, Schmid M, Varga P (2002) Interaction of oxygen with palladium deposited on a thin alumina film. *Surf Sci* 501:270–281
- Storms E (1993) Measurements of excess heat from a Pons–Fleischmann-type electrolytic cell using palladium sheet. *Fusion Technol* 23:230
- Storms E (1996) How to produce the Pons–Fleischmann effect. *Fusion Technol* 29:261
- Storms E, Talcott C (1990) Electrolytic tritium production. *Fusion Technol* 17:680
- Szpak S, Mosier-Boss PA (1996) On the behavior of the cathodically polarized Pd/D system: a response to Vigier's comments. *Phys Lett A* 221:141–143
- Szpak S, Mosier-Boss PA, Smith JJ (1996) On the behaviour of the cathodically polarized Pd/D System: search for emanating radiation. *Phys Lett A* 210:382–390
- Szpak S, Mosier-Boss PA, Boss RD, Smith JJ (1998) On the behavior of the Pd/D system: evidence for tritium production. *Fusion Technol* 33:38–51
- Szpak S, Mosier-Boss PA, Miles MH, Fleischmann M (2004) Thermal behavior of polarized Pd/D electrodes prepared by co-deposition. *Thermochimica Acta* 410:101–107
- Szpak S, Mosier-Boss PA, Young C, Gordon FE (2005a) The effect of an external electric field on surface morphology of co-deposited Pd/D films. *J Electroanal Chem* 580:284–290
- Szpak S, Mosier-Boss PA, Young C, Gordon FE (2005b) Evidence of nuclear reactions in the Pd lattice. *Naturwissenschaften* 92:394–397
- Szpak S, Mosier-Boss PA, Gordon FE (2007) Further evidence of nuclear reactions in the Pd/D lattice: emission of charged particles. *Naturwissenschaften* 94:511–514
- Tsallis C (1988) Possible generalization of Boltzmann–Gibbs statistics. *J Stat Phys* 52:479–487